Cell Stress and Chaperones (2014) 19:105–114
DOI 10.1007/s12192-013-0438-7

ORIGINAL PAPER

Astragaloside IV attenuates glycated albumin-induced epithelial-to-mesenchymal transition by inhibiting oxidative stress in renal proximal tubular cells

Weiwei Qi · Jianying Niu · Qiaojing Qin · Zhongdong Qiao · Yong Gu

Received: 20 March 2013 / Revised: 13 May 2013 / Accepted: 14 May 2013 / Published online: 30 May 2013

Abstract In diabetic kidney disease (DKD), epithelial-to-mesenchymal transition (EMT) is a classic pathological process in tubular damage. Oxidative stress is considered to play an important role in DKD. Astragaloside IV (A-IV), one of the main active ingredients of *Astragalus membranaceus*, exhibits a wide range of biological activities. However, the effect of A-IV on regulating EMT in tubular cells is unclear. This study aims to determine whether A-IV could attenuate glycated albumin (GA)-induced EMT in the NRK-52E cell line by inhibiting oxidative stress. GA and A-IV-induced cytotoxicity were assayed by CCK-8. The intercellular reactive oxygen species (ROS) level was detected by H_2DCFDA. The activity of NADPH oxidase was assayed by adding exogenous NADPH oxidase, and the superoxide dismutase (SOD) units were observed by NBT. We used a microscope to examine the morphology of the NRK-52E cell line. We conducted a wound healing assay to measure cell mobility. To determine mRNA and protein expressions of α-SMA and E-cadherin, we used real-time polymerase chain reaction (real-time PCR), immunofluorescence, and western blot analysis. A-IV significantly attenuated GA-induced amplification of ROS, lowered the increased level of NADPH oxidase activity, and elevated the decreased level of SOD units. The GA-induced NRK-52E cell line showed increased expression of α-SMA and decreased expression of E-cadherin in mRNA and protein levels, whereas A-IV alleviated the expression of α-SMA and increased the expression of E-cadherin. Our data demonstrate that GA could induce NRK-52E cell line EMT through oxidative stress. This effect could be attenuated by A-IV via regulation of the impaired redox balance.

Keywords Astragaloside IV · Glycated albumin · Oxidative stress · EMT · NRK-52E cells

W. Qi · J. Niu · Q. Qin · Y. Gu
Nephrology Department, Shanghai Fifth People's Hospital, Fudan University, Shanghai 200240, China

Z. Qiao
School of Life Science and Biotechnology, Shanghai Jiaotong University, Shanghai 200240, China

Y. Gu (✉)
Nephrology Department, Huashan Hospital, Fudan University, Shanghai 200240, China
e-mail: yonggu@vip.163.com

Introduction

Diabetic kidney disease (DKD) is the most common cause of end-stage renal failure in developed countries (Mogensen 2003). Recently, numerous studies have focused on delineating the pathogenesis of renal fibrosis in chronic kidney disease, including DKD. Research has shown that tubulointerstitial fibrosis is a more consistent predictor of functional impairment than glomerular damage and that epithelial-to-mesenchymal transition (EMT) is a critical step in the pathogenesis of tubulointerstitial fibrosis (Burns and Thomas 2010). The process of EMT demonstrates that epithelial cells lose their characteristics, such as the adherent junction protein E-cadherin, and acquire features and properties that are usually attributed to mesenchymal cells, such as α-smooth muscle actin (α-SMA).

Oxidative stress plays a vital role in the development and progression of DKD (Rösen et al. 2001; Stanton 2011). Increased oxidative stress appears to be the major alteration that drives the activation of cellular pathways in DKD (Gnudi 2012). NADPH oxidase is the major source of reactive oxygen species (ROS) in nonphagocytic cells (Li and Shah 2003). The generation of ROS can be augmented through the increased formation of advanced glycation end-products (AGEs) (Thallas-Bonke et al. 2008), high glucose levels (Ha and Lee 2005), transforming growth factor-β (TGF-β) (Fukawa et al. 2012), and so on. Recent literature

has provided evidence suggesting that free radical generation induces EMT in lung epithelium (Gorowiec et al. 2012). The relationship between EMT and oxidative stress in kidney had been studied in chronic allograft nephropathy (Djamali et al. 2005) and renal proximal tubular epithelial cells induced by TGF-β (Rhyu et al. 2005).

Glucose can react nonenzymatically with the reactive protein amino groups to form labile Schiff bases that subsequently undergo an Amadori rearrangement, resulting in glycated albumin (GA). The intermediate Amadori products may be slowly transformed to AGEs (Kim and Lee 2012). In vivo, the concentration of circulating glycated proteins, driven by the ambient glucose concentration, is increased in diabetes as a result of hyperglycemia (Cohen 2003). A wealth of data support the finding that GA is not only a biomarker for monitoring the fluctuation of glucose levels in 2 to 3 weeks but also an adverse factor in the development of DKD (Cohen et al. 2005). Previous studies (Yoo et al. 2004; Li and Wang 2010) demonstrated that GA induced superoxide generation and stimulated NADPH oxidase activity in mesangial cells. However, little is known about GA-induced EMT by oxidative stress in proximal tubular cells in DKD. Therefore, we aim to clarify whether oxidative stress contributes to GA-induced EMT in NRK-52E cells (rat normal proximal tubular cells).

Astragalus membranaceus, a commonly used Chinese medicinal plant, possesses many pharmacological effects, such as antitumor (Cho and Leung 2007; Li et al. 2012), anti-inflammation (Qin et al. 2012; Lai et al. 2013), and antioxidant functions (Ko et al. 2005; Chen et al. 2011). However, herbal medicine is often categorized as alternative treatment because of the complicated compositions and the lack of scientific evidences to support their benefits. In this study, we investigate the mechanism underlying the reduction of GA-induced EMT in the NEK-52E cell line by astragaloside IV (A-IV). Astragaloside IV (A-IV) is one of the main active ingredients of *A. membranaceus*. Chemically, it is a cycloartane triterpene saponin with a clear formula and definite molecular weight (Lai et al. 2013; Zhao et al. 2013). Yan et al. proved that A-IV was widely distributed to tissues in rats and, of all examined tissues, the kidney has a high concentration distribution (Chang et al. 2012). It was reported that pretreatment with A-IV could ameliorate podocyte apoptosis by attenuating ROS production (Gui et al. 2012) and prevent acute kidney injury by inhibiting oxidative stress (Gui et al. 2013). However, the protective effects of A-IV on oxidative stress and EMT in proximal tubular cells have not been investigated yet. The aim of our study is to assess whether A-IV can attenuate GA-induced EMT in NRK-52E cells by suppressing oxidative stress. Our results will demonstrate the importance of A-IV as a useful antioxidant against tubular damages and provide new insights into the field of DKD therapy.

Materials and methods

Regents

The rat proximal tubular epithelial cell line NRK-52E was purchased from the Institute of Biochemistry and Cell Biology (Shanghai, China). Dulbecco's modified eagle's medium with low glucose (DMEM) was purchased from Gibco (USA). Glycated albumin, 2,7-dichlorodihydrofluorescein diacetate (H_2DCFDA), *N*-acetylcysteine (NAC), apocynin (APO), and Tiron were purchased from Sigma-Aldrich (St. Louis, MO, USA). Diphenyleneiodonium (DPI) and β-nicotinamide adenine dinucleotide phosphate (NADPH) were purchased from Enzo Life Science (Farmingdale, NY, USA). Astragaloside IV (A-IV) (Ronghe Co., Shanghai, China) was dissolved in dimethyl sulfoxide (DMSO) at 5 mg/ml to create a stock solution. Cell counting kit-8 (CCK-8) was purchased from Dojindo (Tokyo, Japan). Total superoxide dismutase (SOD) activity kit was purchased from Beyotime Institute of Biotechnology (Jiangsu, China). Anti-α-SMA and anti-E-cadherin antibodies were obtained from Epitomics (Burlingame, CA, USA). Anti-GAPDH and anti-rabbit IgG were obtained from Cell Signaling Technology (Beverly, MA, USA). FITC secondary antibodies were obtained from Boster (Hubei, China).

Cell culture

Cells were maintained in DMEM (low glucose) supplemented with 5 % fetal bovine serum (FBS) at 37 °C under a humidified 5 % CO_2 atmosphere, containing 100 U/ml penicillin, 100 μg/ml streptomycin, 44 mM $NaHCO_3$, and 14 mM HEPES. Cells were synchronized in FBS-reduced media (0.5 % FBS) for 24 h before the experiments. After this time period, the media were changed to fresh serum-free media with or without various concentrations of GA. In several experiments, we pretreated the cells with antioxidant NAC (0.5 mM), NADPH oxidase inhibitors DPI (2 μM), and APO (20 μM) superoxide scavenger Tiron (1 mM) or A-IV (0.8–80 μg/ml) for 30 min before adding GA.

Assessment of cell viability

Viability of NRK-52E cells was determined by cell counting kit-8 (CCK-8) assay. Cells were seeded at the concentration of 10^5/ml in 96-well plates with FBS-reduced media (0.5 % FBS). After adherence, the cells were stimulated with GA in different concentrations (0–1,000 μg/ml) for different time periods (12, 24, and 48 h). When the effect of A-IV on NRK-52E cell viability was studied, various concentrations of A-IV (0.4 to 80 μg/ml) were added for 24 h. At the end of the exposure, 10 μl of CCK-8 was added to each well and further incubated at 37 °C for 3 h. The absorbance of CCK-8 was detected at 450 nm by a microplate reader. The

viability of the cells was expressed as the fraction of surviving cells relative to untreated controls.

Measurement of intracellular ROS

The fluorescent probe H_2DCFDA was used to assess the generation of intracellular ROS as previously described (Queisser et al. 2011). This compound could be rapidly taken up by the cell and converted by intracellular esterases to 2,7-dichlorodihydrofluorescein (DCF). Cells were cultured in 96-well plates with FBS-reduced media (0.5 % FBS) incubated overnight for adherence. After stimulation with GA for 24 h with or without pretreatment of NAC, DPI, APO, Tiron, or A-IV for 30 min, NRK-52E cells were washed with warm PBS (PH=7.4) and loaded with 10 μM of H_2DCFDA at 37 °C for 30 min. After incubation, cells were rinsed with warm PBS twice, and 100 μl of warm PBS was added per well. We measured the fluorescence emission of DCF using a fluorescence microplate reader with excitation/emission wavelengths set at 485/525 nm. The results of intracellular ROS generation are expressed as percentage fluorescence of the normal cells without GA and A-IV treatments.

Analysis of NADPH oxidase activity

NADPH oxidase activity in cells was measured as previously described (Proell et al. 2007). In brief, cells grown in serum-free medium containing GA in the presence or absence of NAC, DPI, APO, Tiron, or A-IV for 24 h were washed twice in PBS and scraped from the plate in the same solution followed by centrifugation at 12,000*g*, 4 °C, for 3 min, and suspended in PBS, followed by incubation with 250 μmol/l of NADPH. NADPH consumption was monitored by a decrease in absorbance at λ=340 nm for 10 min. For normalization, protein concentration was determined by Bio-Rad Protein Assay reagent. The results were expressed as picomoles per liter of substrate per minute per milligram of protein.

Total SOD assay

The activity of total SOD (T-SOD) for cells was determined using commercially available kits. The T-SOD assay was based on the reduction of nitroblue tetrazolium (NBT) to water insoluble blue formazan. The cells were cultured in six-well plates and GA was added with or without NAC, DPI, APO, Tiron, or A-IV pretreatment for 30 min. We measured the level of T-SOD after a 24-h exposure at the absorbance of 560 nm according to the manufacturer's instructions. Unit of SOD activity was defined as the amount of enzyme required to inhibit the reduction of NBT by 50.0 %. The enzyme activities were expressed as units per milligram of protein.

Cell morphology and wound healing assay

Cells under different conditions were plated in six-well plates at a density of 1×10^5 cells/well. After stimulation for 24 h, morphological changes of NRK-52E cells were observed under an inverted microscope, and images were obtained.

As previously described (Matsuno et al. 2012), NRK-52E cells were seeded onto six-well plates for adherence and scratched using a 200-μl pipette tip after the cells had reached 70 % confluence. The cells were further incubated with or without GA for 24 h. Photomicrographs were obtained using an inverted microscope.

Fluorescence immunocytochemistry

Cells were grown to 70 % confluence in six-well plates and treated in the following manner. The cells were fixed with 4 % paraformaldehyde at room temperature for 30 min, permeabilized using 0.1 % Triton X-100 for 15 min and incubated in a blocking buffer (5 % BSA in PBS, pH7.4) at room temperature for 1 h. Afterward, the cells were incubated with rabbit anti-E-cadherin antibody (1:50) and rabbit anti-α-SMA (1:50) overnight at 4 °C; FITC-conjugated anti-rabbit antibody (1:100) was later added and further incubated in the dark for 60 min at room temperature. A negative control was supplied by incubating cells in IgG instead of primary antibody. In the last 10 min, DAPI solution was added. The cells were observed and photographed using fluorescence microscopy.

Quantitative real-time PCR

Total RNA was isolated by using the AxyPrep™ Multisource Total RNA Miniprep kit (Axygen, USA). An equivalent amount of RNA was converted into complementary DNA (cDNA) with PrimeScript™ RT reagent Kit (Takara, Japan). Subsequently, real-time PCR was performed using an ABI 7500 Sequencing Detection System and SYBR® Premix Ex Taq™ (Takara, Japan). All of the procedures were performed according to the manufacturer's protocols. Cycling condition was as follows: 40 cycles at 95 °C for 5 s and 60 °C for 34 s. The primers used for real-time PCR were as follows: rat α-SMA, 5′-TGTGCTGGACTCTGGAGATG-3′ (forward) and 5′-GAAGGAATAGCCACGCTCAG-3′ (reverse); rat E-cadherin, 5′-AACGAGGGCATTCTGAAAAA-3′ (forward) and 5′-CACTGTCACGTGCAGAATGTACTG-3′ (reverse); rat GAPDH, 5′-GCAAGTTCAATGGCACAG-3′ (forward) and 5′-GCCAGTAGACTCCACGACAT-3′ (reverse). The comparative $2^{-\Delta\Delta CT}$ method was used to calculate the relative expression level of each target gene with GAPDH serving as the housekeeping gene.

Western blotting

At the end of incubation, the cells were washed with PBS and dissolved in lysis buffer that contained protease inhibitor. Equal amounts of proteins in cell homogenates were subjected to 10 % SDS-PAGE and transferred to PVDF membranes. The membranes were blocked with 5 % free fat milk at room temperature for 1 h and then incubated with primary antibody (1:2,000 for rabbit monoclonal anti-α-SMA, #1184-1; 1:2,000 for rabbit monoclonal anti-E-cadherin, #5409-1; 1:2,000 for rabbit monoclonal GAPDH, #2118) at 4 °C overnight; after three washes in TBST, the membranes were incubated with anti-rabbit IgG for 1 h at room temperature. After washing, the signals were visualized using enhanced chemiluminescence (ECL) and X-ray film (Kodak, USA), with GAPDH serving as an internal control.

Statistical analysis

All of the results are expressed as the mean±standard error with n being the number of experiments. Mean, standard deviation (SD), and P values based on the two-tailed t test were calculated with Excel 2007 (Microsoft). $P<0.05$ was considered to be statistically significant.

Results

Effects of GA and A-IV on cell viability

The treatment with GA decreased the cell viability as determined by CCK-8 assay. Cell viability of NRK-52E cells was significantly reduced in a dose-dependent manner after exposure to 0 to 800 μg/ml GA for 24 h (Fig. 1a). Furthermore, exposure to GA (400 μg/ml) induced cell viability decrease in a time-dependent manner (Fig. 1b). At the same time, we found no significant toxicity of A-IV (0.4 to 80 μg/ml) to NRK-52E cells for 24 h (Fig. 2).

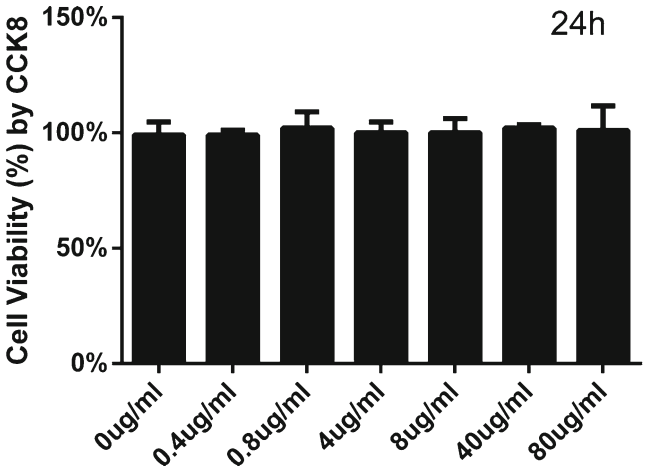

Fig. 2 Effect of A-IV on cell viability. The viability of NRK-52E cells incubated with A-IV was tested by CCK-8 assay. NRK-52E cells were incubated with A-IV at the concentration from 0 to 80 μl/ml for 24 h. The results are expressed as the mean±SD values of three independent experiments

Because of these results and *Astragalus* injection used in the clinic in accordance with specific instruction, we elected to use GA at 0, 200, 400, 600, and 800 μg/ml and A-IV at 0.8, 8, and 80 μg/ml for 24 h in subsequent experiments to determine underlying mechanisms.

A-IV decreased GA-induced intracellular ROS accumulation and NADPH oxidase activity

We measured the intensity of DCF fluorescence to determine the intracellular ROS concentration. We also observed a dose- and time-dependent manner with regard to ROS generation in GA-treated NRK-52E cells (Fig. 3a, b). The significant change was achieved after 24 h of GA treatment from the concentration of 400 μg/ml.

Because NADPH oxidase is an important source of intracellular ROS (Mogensen 2003), we further used NADPH oxidase inhibitors (DPI and Apo) and superoxide

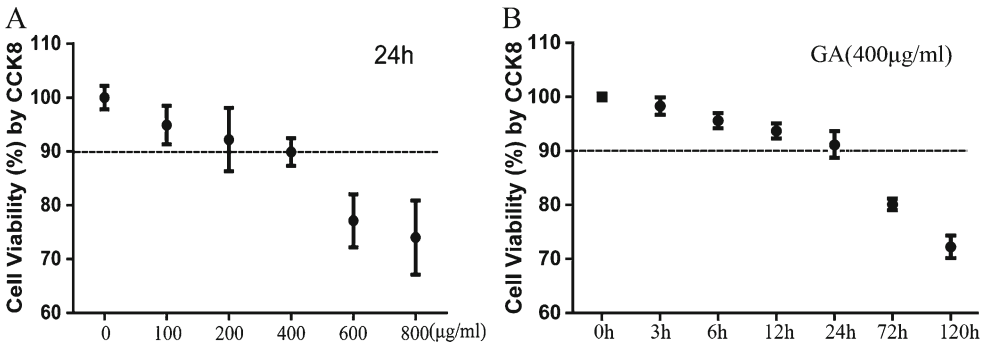

Fig. 1 Effect of GA on cell viability (**a**, **b**). The viability of NRK-52E cells cultured with GA was assessed by performing a CCK-8 assay. **a** NRK-52E cells were stimulated with GA in different concentrations (0–800 μg/ml) for 24 h. **b** NRK-52E cells were incubated for 0–120 h with GA at the concentration of 400 μg/ml. The results are expressed as the mean±SD values of three independent experiments

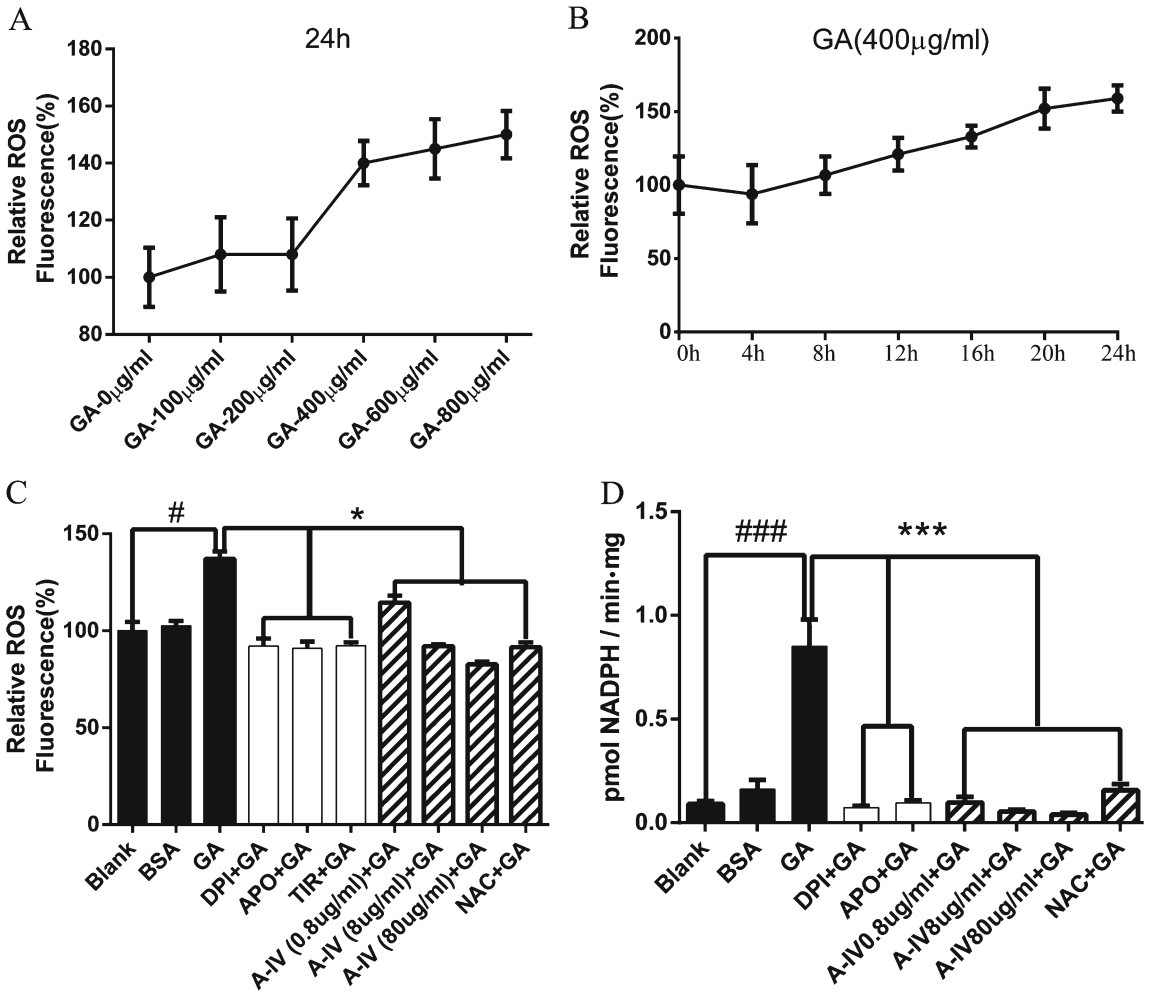

Fig. 3 GA-mediated ROS generation and NADPH oxidase activation were inhibited by A-IV in NRK-52E cells. **a** NRK-52E cells were treated with different concentrations of GA (0–800 μg/ml) for 24 h. **b** NRK-52E cells were incubated for 0–24 h with GA at the concentration of 400 μg/ml. **c** and **d** NRK-52E cells were stimulated by GA (400 μg/ml) for 24 h after pretreatment of NADPH oxidase inhibitors (DPI and Apo) or superoxide scavenger (Tiron) for 30 min and NRK-52E cells were pretreated with different concentrations of A-IV (0.8–80 μg/ml) or antioxidant NAC for 30 min before GA (400 μg/ml) treatment for 24 h. #$P<0.05$ vs. blank; ###$P<0.001$ vs. blank; *$P<0.05$ vs. GA; ***$P<0.001$ vs. GA. Values are expressed as the mean± SD of three independent experiments

scavenger (Tiron) to observe ROS production induced by GA, and we also detected NADPH oxidase activity in GA-treated NRK-52E cells. To determine whether 90 % of the cells could survive, we used CCK-8 to test the concentration of reagents in the current study. As shown in Fig. 3c, NADPH oxidase inhibitors and superoxide scavenger significantly reduced GA-induced DCF-sensitive intracellular ROS generation ($p<0.05$ compared with the GA group).

Considering A-IV to be a potential antioxidant, we primarily detected intracellular ROS level. To assess the antioxidative effect of A-IV, we used NAC, a classic antioxidant, as a positive control. The effect of GA-induced ROS generation in NRK-52E cells was notably decreased by the pretreatment of A-IV and NAC ($p<0.05$ compared with the GA group) and the antioxidative effect of A-IV had a dose-dependent manner (Fig. 3c).

As demonstrated in Fig. 3d, GA increased NADPH oxidase activity in NRK-52E cells ($P<0.001$ compared with the blank group), whereas BSA increased the activity of NADPH oxidase slightly, and there was no significant difference compared with blank group. Two NADPH oxidase inhibitors (DPI and Apo) completely inhibited the GA-mediated increase of NADPH oxidase activation ($P<0.001$ compared with the GA group). As shown in Fig. 2d, preconditioning with 0.8, 8, and 80 μg/ml A-IV or NAC significantly reduced the NADPH oxidase level ($p<0.001$ compared with the GA group).

A-IV enhanced GA-induced intracellular T-SOD reduction

As shown in Fig. 4, treating the cells with GA and BSA for 24 h decreased the intracellular T-SOD levels ($P<0.001$, GA group compared with the blank group; $P<0.05$, BSA group compared with the blank group). As expected, incubation

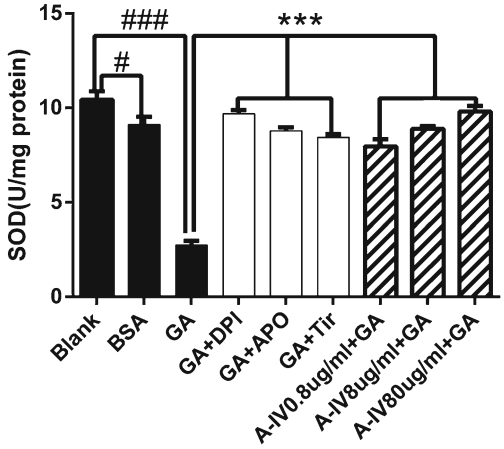

Fig. 4 Effect of A-IV on GA induced the decrease of intracellular T-SOD level. NRK-52E cells were stimulated by GA (400 μg/ml) for 24 h after pretreatment of NADPH oxidase inhibitors (DPI and Apo) and superoxide scavenger (Tiron) for 30 min and NRK-52E cells were pretreated with different concentrations A-IV(0.8–80 μg/ml) or antioxidant NAC for 30 min before GA (400 μg/ml) treatment for 24 h. #P <0.05 vs. blank, ###P<0.001 vs. blank; ***P<0.001 vs. GA. Data are presented as the mean±SD of three independent experiments

with either NADPH oxidase inhibitors (DPI, APO) or superoxide scavenger Tiron (P<0.001 compared with the GA group) significantly attenuated the change in the content of the intracellular T-SOD level. Pretreatment with 0.8, 8, and 80 μg/ml of A-IV and NAC (P<0.001 compared with the GA group) increased the T-SOD level.

A-IV alleviated GA-induced morphological changes and cell mobility

NRK-52E cells displayed typical cobblestone morphology of epithelial cells when the cells were grown in culture medium (Fig. 5a). Exposure to GA for 24 h resulted in a phenotypic conversion from epithelial cells into spindle-shaped fibroblastlike cells (Fig. 5b). With the pretreatment of A-IV (80 μg/ml) for 30 min, a GA-induced phenotypic conversion was significantly lessened (Fig. 5c). Compared to the blank group, NRK-52E cells treated with GA exhibited greater motility, which is one of the characteristics of EMT of renal tubular cells, as determined through a wound healing assay (Fig. 5d and e). A-IV (80 μg/ml) reduced the cell mobility (Fig. 5f).

A-IV inhibited GA-induced EMT in NRK-52E cells

E-cadherin and α-SMA are both tubular EMT markers. We first investigated α-SMA and E-cadherin expression in NRK-52E cells by immunofluorescence assay. We found that GA increased α-SMA expression and suppressed E-cadherin expression significantly (Fig. 6b and e). The administration of A-IV (80 μg/ml) reduced such changes and almost reversed them (Fig. 6c and f).

To determine whether the protection of A-IV on GA-induced EMT was mediated via regulating ROS generation, we observe the effect of NADPH oxidase inhibitors,

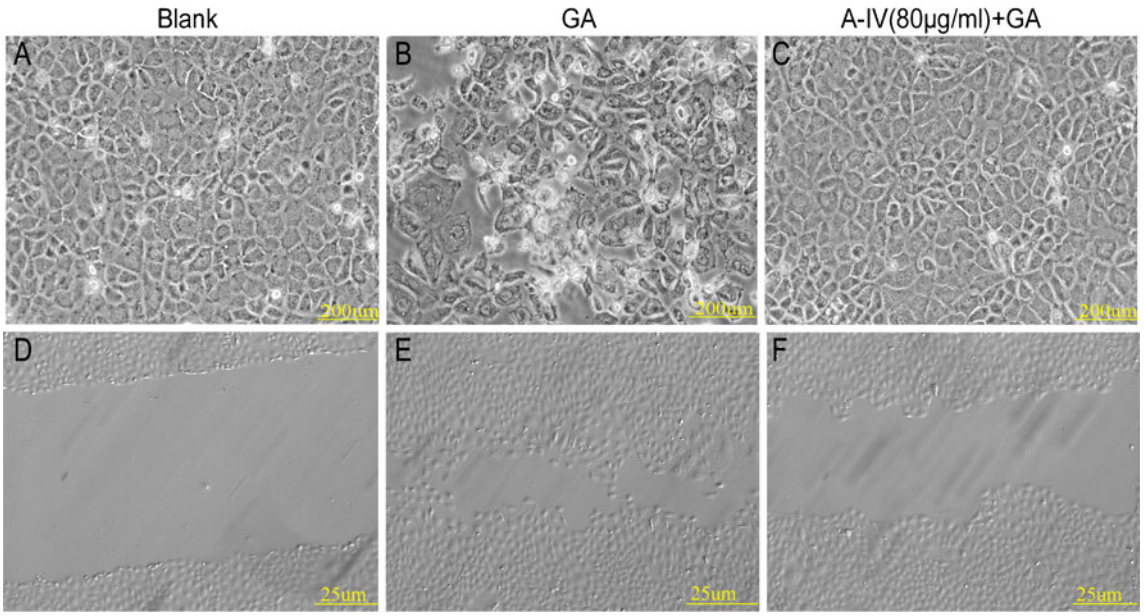

Fig. 5 Effect of A-IV on cell morphological transformation and cellular mobility. A typical epithelial shape of the NRK-52E cells cultured in the blank group (**a**) for 24 h was shown, with the characteristic cobblestone morphology. Exposure to 400 μg/ml GA (**b**) for 24 h induced a phenotypic transition. Pretreatment with 80 μg/ml A-IV for 30 min effectively weakened such changes induced by GA (**c**). Wound healing assay of NRK-52E cells was cultured in **d** the blank group, **e** 400 μg/ml GA group, and **f** GA (400 μg/ml) treating group with A-IV (80 μg/ml) for 24 h. A-IV attenuated the cell mobility caused by GA

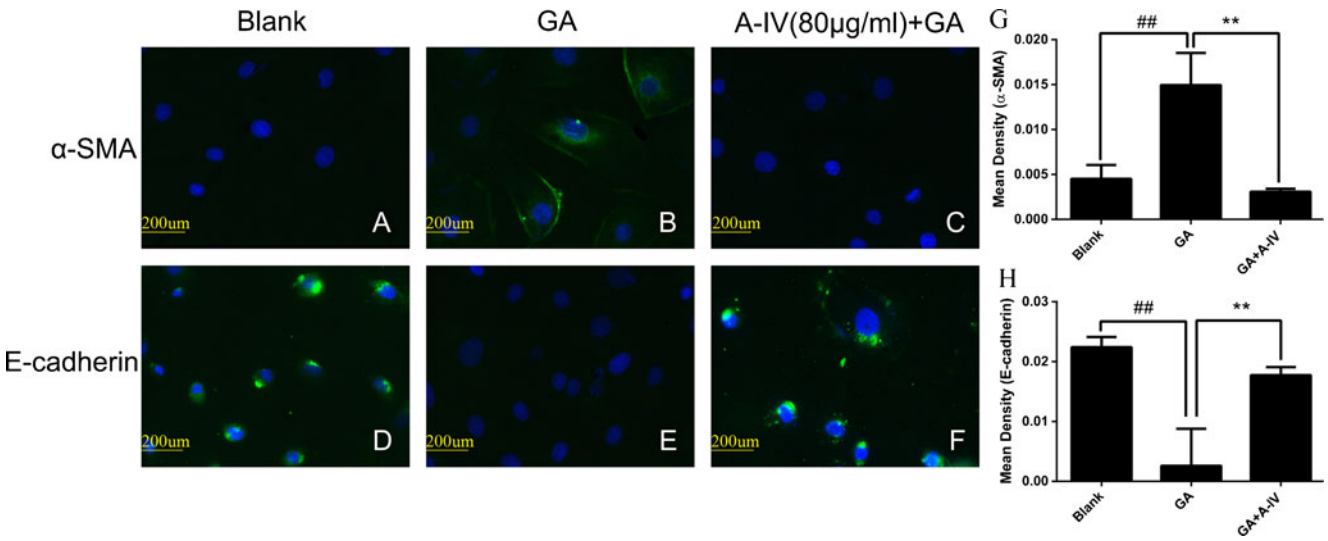

Fig. 6 A-IV inhibited GA-induced EMT in NRK-52E cells. NRK-52E cells were incubated in **a**, **d** the blank group, **b**, **e** 400 μg/ml GA group, **c**, **f** GA (400 μg/ml) treating group with A-IV (80 μg/ml) for 24 h. The effects of A-IV protective effect on α-SMA and E-cadherin expressions were assessed by immunofluorescent microscopy. **g**, **h** Semiquantitative fluorescence intensity for α-SMA and E-cadherin expression in blank group, 400 μg/ml GA group, and GA (400 μg/ml) treating group with A-IV (80 μg/ml). Images were obtained in at least three independent experiments. ×400

superoxide scavenger, NAC, and different concentrations of A-IV on GA-induced EMT. We first examined the mRNA expression of EMT biomarkers in NRK-52E cells (Fig. 7a and b). The GA-treated cells significantly increased the mRNA expression of α-SMA and reduced the mRNA expression of E-cadherin ($P<0.01$ compared with the blank group). Moreover, NADPH oxidase inhibitors (DPI and APO), superoxide scavenger Tiron, A-IV, and NAC, abolished the changes induced by GA to different degrees ($P<0.01$ compared with the GA group). Simultaneously, the effects of A-IV presented a dose-dependent manner in mRNA expression. Similar alterations were observed in protein expressions (Fig. 7c, d, e, and f). Thus, these results suggest that GA-induced EMT in NRK-52E cells via oxidative stress, and A-IV has a potential protective effect on oxidative stress-induced EMT.

Discussion

Experimental and clinical studies have suggested that oxidative stress plays a critical role in the pathogenesis and progression of diabetic complications (Rösen et al. 2001; Stanton 2011). Accumulating evidence indicated that increased concentrations of GA contribute to the development of DKD (Cohen et al. 2005; Yoo et al. 2004; Li and Wang 2010). Because GA presents a latent risk factor in many tissues (Zhang et al. 2006; Hattori et al. 2001), including causing oxidative stress injury in cardiac myocytes (Zhang et al. 2006) and mesangial cells (Li and Wang 2010), we hypothesized that GA might cause oxidative stress in proximal tubular cells.

ROS include oxygen radicals, such as the superoxide anion ($O^{2\bullet-}$), and the hydroxyl radical (OH•), and also some not-radical derivatives of oxygen, such as hydrogen peroxide (H_2O_2) (Cossarizza et al. 2009). ROS can be generated within living cells by the following major sources such as mitochondria, plasma membrane NADPH oxidase, or several enzymes involved in redox reactions (Li and Shah 2003). Recent studies indicated that NADPH oxidase was a major source of ROS production in many nonphagocytic cells, including vascular smooth muscle cells (Perez-Vizcaino et al. 2010), endothelial cells (Montezano and Touyz 2012), renal mesangial cells, and tubular cells (Li and Shah 2003). Under physiologic conditions, NADPH oxidase has very low-level constitutive activity. However, NADPH oxidase activity can be upregulated both acutely and chronically in response to stimuli such as growth factors, cytokines, high glucose, and hyperlipidemia (Li and Shah 2003). In our present study, we confirmed that GA increased intracellular ROS expression in a dose- and time-dependent manner in NRK-52E cells (Fig. 3a and b). Because both DPI and APO are not selective inhibitors of NADPH oxidase, we used DPI and APO to overcome this limitation. NADPH oxidase inhibitors (DPI and APO) and superoxide scavenger (Tiron) significantly reduced GA-induced generation of intracellular ROS to a similar extent, which suggests that NADPH oxidase is an important source of GA-induced intracellular ROS in NRK-52E cells (Fig. 3c).

In normal conditions, cells are often equipped with several antioxidant defense systems to prevent ROS damage, such as uric acid, ascorbic acid, sulfhydryl-containing molecules, and antioxidant enzymes. SOD is a kind of enzyme

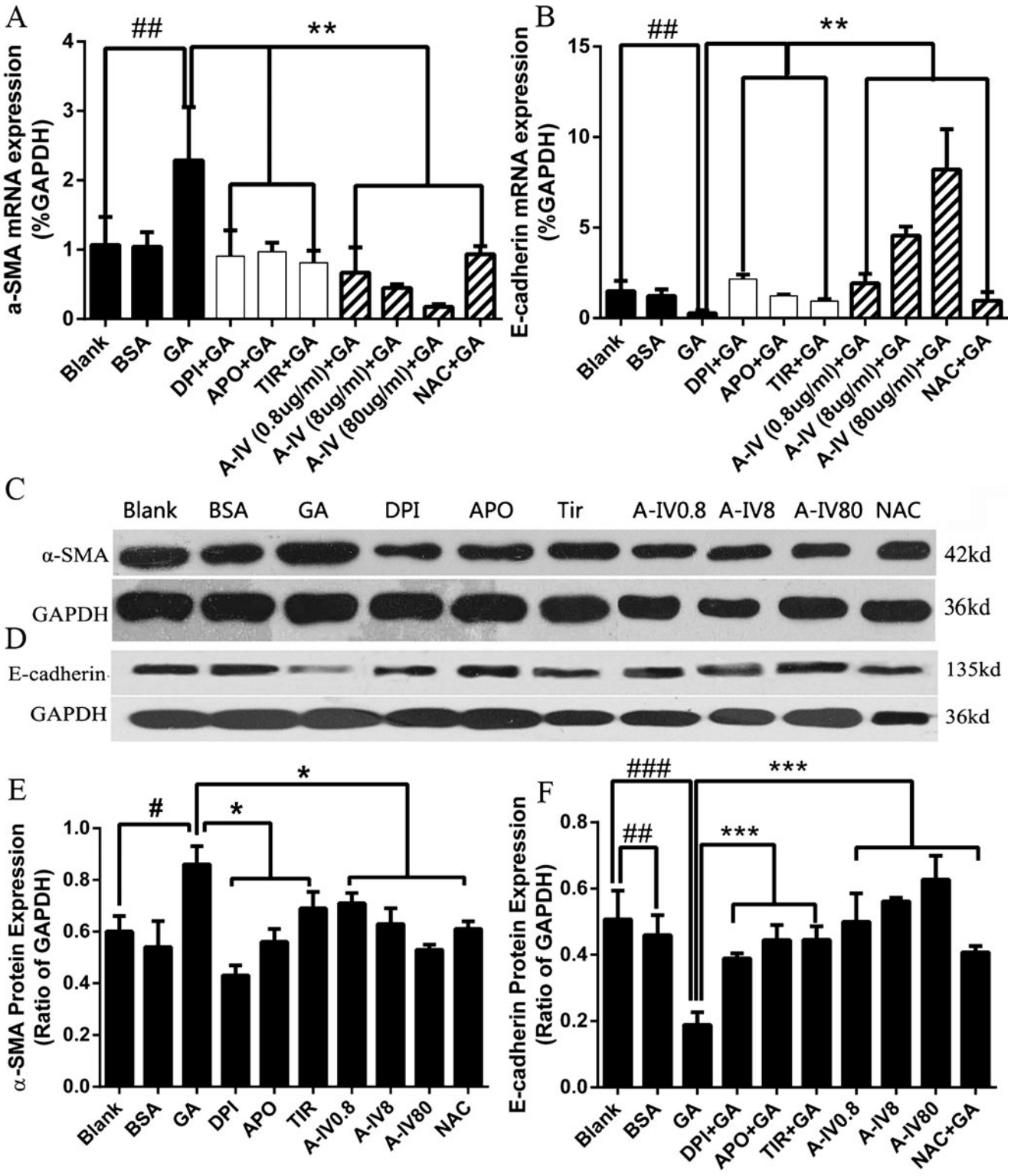

Fig. 7 Effect of A-IV on the GA-induced EMT in NRK-52E. Real-time PCR revealed GA increased α-SMA (**a**) and reduced E-cadherin (**b**) mRNA expressions dramatically, whereas NADPH oxidase inhibitors and different concentrations of A-IV weakened such changes. Similar results were observed through western blotting analysis (**c**, **d**, **e**, **f**). #$P<0.05$, ##$P<0.01$, ###$p<0.001$ vs. blank; *$P<0.05$, **$P<0.01$, ***$P<0.001$ vs. GA. Values are expressed as the mean±SD of three independent experiments

included in antioxidant defenses (West 2000). The reaction from $O^{2\bullet-}$ to H_2O_2 can be spontaneous or it can be catalyzed by SOD. It was considered that hyperglycemia could lower the activity of SOD in patients with diabetes (Shen et al. 2012). In the present study, GA treatment led to a decrease of intracellular T-SOD content, and this reduction was attenuated by the pretreatment with NADPH oxidase inhibitors in NRK-52E cells (Fig. 4).

EMT is a biological process in which the epithelial cells undergo several biochemical alterations that permit the achievement of a mesenchymal phenotype. Presently, we acknowledge that EMT plays a role in the process of organ fibrosis (Cannito et al. 2010). Tubular epithelial cells of the adult kidney are known to transform into mesenchymal phenotype in disease states, thereby undergoing EMT. Various stimuli, such as high glucose, profibrotic cytokines, and inflammatory mediators, trigger pathways to activate transcription factors of tubular epithelial cells, which, in turn, induce phenotypic transformation (Strutz 2009). Our study demonstrates that GA resulted in EMT changes characterized by advancing cellular mobility and morphological transformation (Fig. 5), decreasing expression of E-cadherin, and enhancing expression of α-SMA (Figs. 6 and 7) in NRK-52E cells. However, the direct role of EMT in the tubular epithelial cells and oxidative stress is less well studied. To the best of our knowledge, our investigation is the first study to demonstrate that GA-induced oxidative stress causes the generation of EMT in NRK-52E cells. We observed GA-induced changes of EMT as early as 24 h of stimulation and noted that they were blocked by the NADPH oxidase inhibitors and superoxide scavenger, which suggests that GA-induced oxidative stress was responsible for EMT.

A. membranaceus, a traditional Chinese herbal medicine, has been widely used in clinical practice in the form of *Astragalus* injection (Ko et al. 2005; Qin et al. 2012). However, the ingredients of *Astragalus* injection are too numerous for the medicine to have an easily explained mechanism. Thus, we decided to use A-IV, which is one of the main active ingredients of *A. membranaceus* with clear formula and molecular weight, as the potential antioxidant in our study. According to the instructions for Astragalus injection, we used A-IV concentrations that ranged from 0.4 to 80 μg/ml to test the cell viability. The result showed that there was no significant toxicity among these concentrations (Fig. 2). In the following experiments, we chose 0.8, 8, and 80 μg/ml as the test concentrations to observe the antioxidative effect of A-IV. As expected, we found that A-IV effectively reduced the intracellular ROS level (Fig. 3c), inhibited NADPH oxidase activity (Fig. 3d), and increased intracellular T-SOD level (Fig. 4) induced by GA in a dose-dependent manner, which was similar to the effect of NAC, a classical antioxidant. These results suggested that the antioxidative stress of A-IV might be related to the inhibition of NADPH oxidase activity. Additionally, we observed that A-IV dramatically reversed the expression of E-cadherin and α-SMA induced by GA as well as NAC in NRK-52E (Fig. 7). These data demonstrated that A-IV could inhibit GA-induced EMT by reducing oxidative stress impairment. This strong evidence supports the potential that A-IV might play a significant role as an antioxidant that can resist oxidative damages.

Conclusions

Our data indicate that GA caused oxidative stress and resulted in EMT in NRK-52E cells. A-IV exhibited protective action against GA-induced EMT of NRK-52E cells by repairing redox imbalance, which might be beneficial in the prevention of tubulointerstitial fibrosis in patients with diabetic kidney disease.

Acknowledgments This work was supported by a grant from the Major State Basic Research Development Program of China (973 Program) (2012CB517700), the Key Basic Research Project of the Science and Technology Commission of Shanghai Municipality (10JC1413000), and the National Natural Science Foundation of China (30871175).

Conflict of interest None.

References

Burns WC, Thomas MC (2010) The molecular mediators of type 2 epithelial to mesenchymal transition (EMT) and their role in renal pathophysiology. Expert Rev Mol Med 27:12–17

Cannito S, Novo E, di Bonzo LV, Busletta C, Colombatto S, Parola M (2010) Epithelial–mesenchymal transition: from molecular mechanisms, redox regulation to implications in human health and disease. Antioxid Redox Signal 12:1383–430

Chang YX, Sun YG, Li J, Zhang QH, Guo XR, Zhang BL et al (2012) The experimental study of *Astragalus membranaceus* on meridian tropsim: the distribution study of astragaloside IV in rat tissues. J Chromatogr B Analyt Technol Biomed Life Sci 12(911):71–5

Chen R, Shao H, Lin S, Zhang JJ, Xu KQ (2011) Treatment with *Astragalus membranaceus* produces antioxidative effects and attenuates intestinal mucosa injury induced by intestinal ischemia–reperfusion in rats. Am J Chin Med 39:879–87

Cho WC, Leung KN (2007) In vitro and in vivo anti-tumor effects of *Astragalus membranaceus*. Cancer Lett 252:43–54

Cohen MP (2003) Intervention strategies to prevent pathogenetic effects of glycated albumin. Arch Biochem Biophys 419:25–30

Cohen MP, Chen S, Ziyadeh FN, Shea E, Hud EA, Lautenslager GT et al (2005) Evidence linking glycated albumin to altered glomerular nephrin and VEGF expression, proteinuria, and diabetic nephropathy. Kidney Int 68:1554–61

Cossarizza A, Ferraresi R, Troiano L, Roat E, Gibellini L, Bertoncelli L et al (2009) Simultaneous analysis of reactive oxygen species and reduced glutathione content in living cells by polychromatic flow cytometry. Nat Protoc 4:1790–7

Djamali A, Reese S, Yracheta J, Oberley T, Hullett D, Becker B (2005) Epithelial-to-mesenchymal transition and oxidative stress in chronic allograft nephropathy. Am J Transplant 5:500–9

Fukawa T, Kajiya H, Ozeki S, Ikebe T, Okabe K (2012) Reactive oxygen species stimulates epithelial mesenchymal transition in normal human epidermal keratinocytes via TGF-beta secretion. Exp Cell Res 318:1926–32

Gnudi L (2012) Cellular and molecular mechanisms of diabetic glomerulopathy. Nephrol Dial Transplant 27:2642–9

Gorowiec MR, Borthwick LA, Parker SM, Kirby JA, Saretzki GC, Fisher AJ (2012) Free radical generation induces epithelial-to-mesenchymal transition in lung epithelium via a TGF-β1-dependent mechanism. Free Radic Biol Med 52:1024–32

Gui D, Guo Y, Wang F, Liu W, Chen J, Chen Y et al (2012) Astragaloside IV, a novel antioxidant, prevents glucose-induced podocyte apoptosis in vitro and in vivo. PLoS One 7:e39824

Gui D, Huang J, Liu W, Guo Y, Xiao W, Wang N (2013) Astragaloside IV prevents acute kidney injury in two rodent models by inhibiting oxidative stress and apoptosis pathways. Apoptosis 18:409–22

Ha H, Lee HB (2005) Reactive oxygen species amplify glucose signaling in renal cells cultured under high glucose and in diabetic kidney. Nephrology (Carlton) 10 Suppl:S7-10.

Hattori Y, Kakishita H, Akimoto K, Matsumura M, Kasai K (2001) Glycated serum albumin-induced vascular smooth muscle cell proliferation through activation of the mitogen-activated protein kinase/extracellular signal-regulated kinase pathway by protein kinase C. Biochem Biophys Res Commun 281:891–6

Kim KJ, Lee BW (2012) The roles of glycated albumin as intermediate glycation index and pathogenic protein. Diabetes Metab J 36:98–107

Ko JK, Lam FY, Cheung AP (2005) Amelioration of experimental colitis by *Astragalus membranaceus* through anti-oxidation and inhibition of adhesion molecule synthesis. World J Gastroenterol 11:5787–94

Lai PK, Chan JY, Cheng L, Lau CP, Han SQ, Leung PC et al (2013) Isolation of anti-inflammatory fractions and compounds from the root of *Astragalus membranaceus*. Phytother Res 27:581–7

Li JM, Shah AM (2003) ROS generation by nonphagocytic NADPH oxidase: potential relevance in diabetic nephropathy. J Am Soc Nephrol 14(8 Suppl 3):S221–6

Li Y, Wang S (2010) Glycated albumin activates NADPH oxidase in rat mesangial cells through up-regulation of p47phox. Biochem Biophys Res Commun 397:5–11

Li Q, Bao JM, Li XL, Zhang T, Shen XH (2012) Inhibiting effect of *Astragalus* polysaccharides on the functions of CD4+CD25 high Treg cells in the tumor microenvironment of human hepatocellular carcinoma. Chin Med J (Engl) 125:786–93

Matsuno Y, Coelho AL, Jarai G, Westwick J, Hogaboam CM (2012) Notch signaling mediates TGF-β1-induced epithelial-mesenchymal transition through the induction of Snai1. Int J Biochem Cell Biol 44:76–89

Mogensen CE (2003) Microalbuminuria and hypertension with focus on type 1 and type 2 diabetes. J Intern Med 254:45–66

Montezano AC, Touyz RM (2012) Reactive oxygen species and endothelial function—role of nitric oxide synthase uncoupling and Nox family nicotinamide adenine dinucleotide phosphate oxidases. Basic Clin Pharmacol Toxicol 110:87–94

Perez-Vizcaino F, Cogolludo A, Moreno L (2010) Reactive oxygen species signaling in pulmonary vascular smooth muscle. Respir Physiol Neurobiol 174:212–20

Proell V, Carmona-Cuenca I, Murillo MM, Huber H, Fabregat I, Mikulits W (2007) TGF-beta dependent regulation of oxygen radicals during transdifferentiation of activated hepatic stellate cells to myofibroblastoid cells. Comp Hepatol 6:1

Qin Q, Niu J, Wang Z, Xu W, Qiao Z, Gu Y (2012) *Astragalus membranaceus* inhibits inflammation via phospho-P38 mitogen-activated protein kinase (MAPK) and nuclear factor (NF)-κB pathways in advanced glycation end product-stimulated macrophages. Int J Mol Sci 13:8379–87

Queisser N, Schupp N, Stopper H, Schinzel R, Oteiza PI (2011) Aldosterone increases kidney tubule cell oxidants through calcium-mediated activation of NADPH oxidase and nitric oxide synthase. Free Radic Biol Med 51(11):1996–2006

Rhyu DY, Yang Y, Ha H, Lee GT, Song JS, Uh ST et al (2005) Role of reactive oxygen species in TGF-beta1-induced mitogen-activated protein kinase activation and epithelial–mesenchymal transition in renal tubular epithelial cells. J Am Soc Nephrol 16:667–75

Rösen P, Nawroth PP, King G, Möller W, Tritschler HJ, Packer L (2001) The role of oxidative stress in the onset and progression of diabetes and its complications: a summary of a Congress Series sponsored by UNESCO-MCBN, the American Diabetes Association and the German Diabetes Society. Diabetes Metab Res Rev 17:189–212

Shen XP, Li J, Zou S, Wu HJ, Zhang Y (2012) The relationship between oxidative stress and the levels of serum circulating adhesion molecules in patients with hyperglycemia crises. J Diabetes Complications 26:291–5

Stanton RC (2011) Oxidative stress and diabetic kidney disease. Curr Diab Rep 11:330–6

Strutz FM (2009) EMT and proteinuria as progression factors. Kidney Int 75:475–81

Thallas-Bonke V, Thorpe SR, Coughlan MT, Fukami K, Yap FY, Sourris KC et al (2008) Inhibition of NADPH oxidase prevents advanced glycation end product-mediated damage in diabetic nephropathy through a protein kinase C-alpha-dependent pathway. Diabetes 57:460–9

West IC (2000) Radicals and oxidative stress in diabetes. Diabet Med 17:171–80

Yoo CW, Song CY, Kim BC, Hong HK, Lee HS (2004) Glycated albumin induces superoxide generation in mesangial cells. Cell Physiol Biochem 14:361–8

Zhang M, Kho AL, Anilkumar N, Chibber R, Pagano PJ, Shah AM et al (2006) Glycated proteins stimulate reactive oxygen species production in cardiac myocytes: involvement of Nox2 (gp91phox)-containing NADPH oxidase. Circulation 113:1235–43

Zhao M, Zhao J, He G, Sun X, Huang X, Hao L (2013) Effects of astragaloside IV on action potentials and ionic currents in guinea-pig ventricular myocytes. Biol Pharm Bull 36:515–21